IEEE Access
Multidisciplinary | Rapid Review | Open Access Journal

Received November 4, 2021, accepted November 16, 2021, date of publication November 19, 2021,
date of current version December 3, 2021.

Digital Object Identifier 10.1109/ACCESS.2021.3129516

A Study Toward Appropriate Architecture of System-Level Prognostics: Physics-Based and Data-Driven Approaches

SEOKGOO KIM[1,2], NAM HO KIM[1], AND JOO-HO CHOI[2]
[1]Department of Mechanical & Aerospace Engineering, University of Florida, Gainesville, FL 32611, USA
[2]Department of Aerospace & Mechanical Engineering, Korea Aerospace University, Goyang-si 10540, Republic of Korea

Corresponding author: Joo-Ho Choi (jhchoi@kau.ac.kr)

This work was supported by the Korea government (Ministry of Science and ICT: MSIT) through the National Research Foundation of Korea (NRF) under Grant 2020R1A4A4079904.

ABSTRACT Many existing studies have investigated component-level Prognostics and Health Management (PHM) problems. In the real field, the PHM for the system is more important, which deals with the exploration of the system health derived from components degradations, from which the decision can be made to which components to repair. While there have been few recent studies in this direction, no studies are found that have investigated this issue from the systems perspective. Motivated by this, appropriate architecture for the system-level PHM is proposed for the physics-based and data-driven approaches. The architecture is demonstrated using a direct current (DC) motor system, which addresses the system health by the degradation of two components: bearing and permanent magnet. Due to the lack of real field data, simulation data are made using the motor dynamic equation. The two approaches are compared from the perspective of model construction and required information. In conclusion, the proposed architecture enables the estimation of components and system health, as well as the prediction of their remaining useful life. Furthermore, a what-if study allows us to investigate how long the system can be operated by repairing each component, from which the optimum maintenance plan can be made.

INDEX TERMS Architectures, system-level prognostics, physics-based approach, data-driven approach, remaining useful life (RUL), DC motor system.

I. INTRODUCTION

In the industry, prediction of upcoming failure or remaining useful life (RUL) brings a lot of advantages, such as economic benefits and safe system operation. For this reason, numerous researches have been made for Prognostics and Health Management (PHM) not only by the academic researchers but also the industrial engineers, and there are many review papers for numerous topics under various perspectives (see, e.g., [1], [2]). Up to date, however, most of the existing approaches have focused on the component-level PHM, such as the bearing [3]–[7], battery [8], [9], and gear [10]–[13].

In practice, an engineering system consists of multiple components, and they are designed to perform a specific function, which we call the system performance. Since the components within the system interact with each other, their degradations may often affect the system's performance in a complex manner. In other words, various outputs from different components contribute as inputs for a system model that calculates the performance of the target system. Depending on the existence of the physical model, system performance can be defined by a physical parameter reflecting the health condition of the system, virtual health index obtained from machine learning algorithm, or system failure probability of multiple components. In this sense, the major challenge of the system-level PHM, as opposed to the component-level, is to understand the inter-relation between the system and components. Once configured properly, the next steps may be (1) exploration of the system health due to the components degradations, (2) inference of health of the components and system performances, and (3) prediction of the components life against the system failure threshold.

Due to its complexity, much fewer studies have been made in the literature for the system-level PHM. Similar to the

The associate editor coordinating the review of this manuscript and approving it for publication was Chong Leong Gan.

component PHM, the system PHM can be grouped into physics-based and data-driven approaches. Physics-based approaches utilize the system dynamic model that identifies the relationship between components and system. Daigle *et al.* [14] proposed a model decomposition approach to reduce the computational expense occurring in physics-based prognostics. They have decomposed the system model into a set of local sub-models suitable for prognostics, which is computationally independent. As a result, the system RUL was determined by the minimum life of the decomposed models. Daigle and Goebel [15] have predicted system RUL by employing the particle filter (PF) algorithm to estimate the joint state parameters when multiple damage progressions exist. Vasan *et al.* [16] suggested that the system should be decomposed into multiple critical parts and exploit parameters specific to the system to predict the RUL. Although the above-mentioned researches have shown successful prognostic performance, system RUL is simply determined by the minimum RUL of the individual components.

Considering that the system performance is characterized by the combined effects of components, the system RUL should be determined based on the system health itself and the components RUL should be decided dependent on this. For this purpose, Khorasgani *et al.* [17] proposed two-step processes, the estimation and prediction: (1) system state variables and degradation parameters of the system model are estimated by the PF, and (2) stochastic simulation and inverse-FORM are used to predict the system RUL. More recently, Tamssaouet *et al.* [18], [19] have proposed system-level prognostics using an inoperability input-output model (IIM) to account for the interactions between their components, which is originated from the economic flows analysis. However, it is highly difficult to develop such a system model, whether it is physics-based or economic-based, which requires a comprehensive understanding of the system.

To overcome this limitation, data-driven approaches have been employed, which may fall into two main streams. The first is the direct RUL method, which aims to train artificial intelligence (AI) algorithm, mapping the measured data into the RUL of the target system. For this purpose, the turbofan engine degradation simulation data set made by Commercial Modular Aero-Propulsion System Simulation (CMAPSS) code has been used in many references. Several algorithms have been applied to predict the RUL of aircraft engines using the data, such as the multi-layer perceptron (MLP) [20], [21], convolutional neural network (CNN) [22], recurrent neural network (RNN) [23], and long short-term memory (LSTM) [24]–[26]. The second method is to predict the virtually defined system performance that degrades from 0 (at the early stage) to 1 (close to the end-of-life). As the system performance is defined by a single health parameter, relevant algorithms have been used to predict the RUL, such as the particle filter [27], similarity-based method [28], [29], and ensemble approach [30]. Although the data-driven approaches do not require the physical model, there are two challenges to discuss: First, it usually suffers from the lack of run-to-fail data to train the model. Despite some remedial efforts to overcome this, it remains the biggest obstacle in this approach [31]–[33]. The second, which is more important, is that many data-driven approaches treat the system as a black box, which is no longer the system-level approach since it does not provide any information for the degradation and RUL of individual components. As a result, the system is treated simply as another version of a large-scale component. Under this approach, one can only replace the whole system when failure is imminent, which is of only marginal value. In order to achieve a proper system-level PHM, the algorithm should be able to perform the diagnosis and prognosis for the components and system simultaneously.

Figure. 1 illustrates an ideal concept of system-level PHM to be pursued in this paper. First, operation and sensors signals are acquired over the cycles of operation, which are used to construct a digital system for the PHM via physics-based or data-driven approaches. Then the constructed system is used to assess the current health state of the system as well as the components and to predict their RULs. It is important that the RULs of the components should be determined conditional on the RUL of the system. Once the RULs are obtained, they are applied to the maintenance plan. For example in the figure, the current health of the three components are 40, 20 and 60 % against their thresholds, whereas the RULs are 10, 40 and 20 cycles, respectively. Note that although component 3 is the most degraded, it has a longer RUL than component 1 due to its slower degradation rate. As a result, component 1 should be replaced after 10 cycles since it is the earliest threat to system failure. After the maintenance, however, the system health is not restored to the complete normal since the others are still in degraded conditions.

In our opinion, this is the ideal solution that meets the original goal of the system PHM. In order to implement this in reality, different information are needed depending on the approaches. A physics-based approach requires the system dynamics describing the behavior or interconnection between the system and components. A data-driven approach requires the maintenance data which have recorded components degradations and corresponding system performance over cycles until failure. Therefore, each approach has its own strengths and weaknesses. To the author's knowledge, no literature has addressed the system PHM in this perspective. Motivated by this, this paper proposes an appropriate architecture for conducting the physics-based and data-driven system PHMs and analyzing their pros and cons. Unfortunately, it is difficult to find the real data for the system and components that meet this purpose. Instead, a DC motor system is employed to illustrate the concept and methods, in which two components, a bearing and a permanent magnet, deteriorate the system performance, which is given as the output torque in this study. Simulations are carried out using the motor dynamic equations, in which the components are artificially degraded over cycles, and virtual measurements are made accordingly.

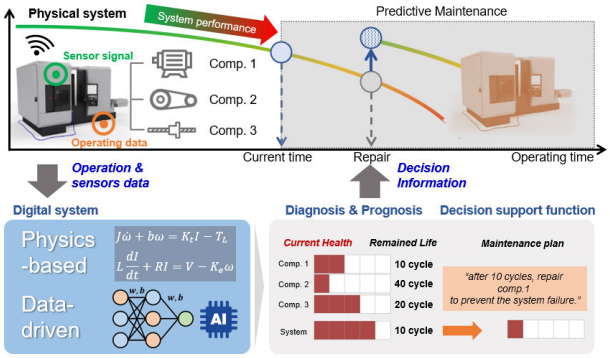

FIGURE 1. System-level prognostics and health management.

II. METHODOLOGY

A. PHYSICS-BASED APPROACH WITH SYSTEM DYNAMIC MODEL

The physics-based approach employs a physical model for the purpose of fault diagnosis and prognosis. Fig. 2 describes the proposed architecture of the physics-based approach, which consists of two phases: construction of the system dynamics model on the left and PHM implementation on the right.

In the model construction, the system model is developed via suitable simulation tools or algorithms such as Simulink, lumped parameters, Bond graph, etc. During the model construction, a group of parameters is identified, where inputs are the operation parameter u and health parameter h of critical components affecting the system degradation. Outputs are the state variable x, system performance S and measurement z to estimate the current health state of the system and components. Three models are established, which are the state model for x usually given by a recursive form in the time domain, the measurement model relating the state with the measurement, and the performance model of the system. These three models are defined as

$$\dot{x} = f(x, h, u) \tag{1}$$

$$z = g(x, h) \tag{2}$$

$$S = sys(x) \tag{3}$$

The PHM implementation phase consists of two parts: online estimation and diagnosis in the upper-right figure and offline training and prognosis in the lower-right figure. In online estimation, the state x in a single cycle is estimated for the input operation parameter u, from which the system performance S is evaluated by the performance model. Depending on the availability of health parameter h, the online estimation phase comprises of two stages. In the first stage named estimation stage, h and x are estimated as an unknown using the measured data z. Unknown parameters are priorly estimated by the state model and updated by the measurement model. In the prediction stage, h is known as a priori while there are no measurements. In this case, h is input to predict the state x only. In both stages, the system performance is computed using the obtained state x. If the measurement z is obtained in every cycle, the cumulated health parameters $h_{0:k}$, from the beginning to the current cycle k, can be estimated at the estimation stage. Then they are transferred to off-line training and prognosis. In order to describe the degradation trend more efficiently, the health parameters are usually fitted either by a physical model or an empirical model:

$$h_{cyc} = d\,(t, \theta | h_{0:k}) \tag{4}$$

where h_{cyc} denotes the health parameters as a function of cycles, d is its mathematical model, θ is the model parameters, and t is the cycle. Once the model is fitted by $h_{0:k}$ up to the current cycle, it can be extrapolated to predict h in the future. The predicted h is transferred to the prediction stage, from which the state x and the system performance S in the future are predicted. The predicted S is transferred to the off-line training phase to obtain the future evolution of the system performance, as matched with those of the health parameter h in the future. Upon examining the RUL of the system performance against the failure threshold, one can identify the most critical health parameter (i.e., component) that leads to the earliest system failure and its remaining cycles, which is valuable information in maintenance management.

The overall procedure is summarized in Fig. 3, in which the highlighted parts are those different from the data-driven approach addressed in the next section. For the implementation phase, the online estimation and diagnosis part of Fig. 2 can be best accommodated by the Bayesian approach such as the Extended Kalman or Particle Filter algorithms. Then the health parameter h and state x are estimated in the form of distribution such as the mean and covariance or the samples, which reflect the uncertainty in the process. The offline training and prognosis part can also be performed similarly, but a simpler linear/nonlinear regression can also be employed to this end. The degradation model parameter θ in $d(\cdot)$ are estimated based on the accumulated values $h_{0:k}$ until the current cycles. Then the degradation in the future is predicted by θ with uncertainty, which is usually expressed by the confidence bounds in the result.

B. DATA-DRIVEN APPROACH WITH MAINTENANCE INFORMATION

When a domain knowledge or physical model for the target asset is absent, a data-driven approach is the only option. As shown in Fig. 4, which is similar to the physics-based approach, the architecture consists of the construction (left) and implementation (right) phases. In the construction phase, an empirical model is constructed using a proper machine learning algorithm such as artificial neural networks or Gaussian process regression. Preliminary steps such as fault tree analysis, functional block diagram, or Bayesian network can be employed, if necessary, to identify the hierarchical structure with causal effect relations between the component health and system performance. As in the physics-based approach, the model consists of input operation parameter u,

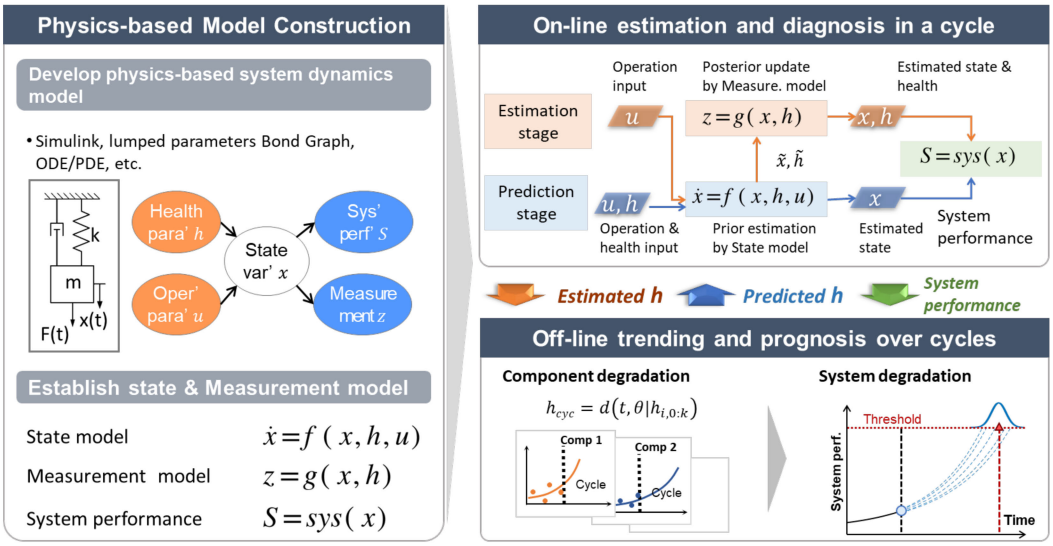

FIGURE 2. Architecture for physics-based approach.

Construction phase (left figure)	
• Establish state, measurement, and performance model, as given in (1)-(3)	
Implementation phase (right figure)	
• Estimate health parameter h and state x using the measurement z.	Estimation stage in upper figure
• Transfer estimated data $h_{0:k}$ up to the current cycle to offline trending.	
• Fit the data $h_{0:k}$ to degradation model (4) and extrapolate h to predict the future degradation.	Left part of lower figure
• Transfer predicted health parameters h in the future to online estimation.	
• Predict state x and system performance S using h in the future.	Prediction stage in upper figure
• Transfer predicted S in the future to offline trending.	
• Determine the remaining life of S against failure threshold.	Right part of lower figure

Note the colored parts in the figure are different from data-driven approach.

FIGURE 3. Overall procedure for physics-based approach as illustrated in Figure 2.

health parameter h of components, system performance S, and feature f_z derived from measurements z. As opposed to the physics-based approach, measurement z are not used directly but transformed into the features to use in the machine learning, which usually requires substantial domain knowledge and expertise:

$$f_z = fe(z, u) \tag{5}$$

where fe denotes the feature extraction as a function of raw measurement signal z and operation parameter u. Here, state variable x is not considered due to the lack of underlying physics. Regarding the health parameter h, a large amount of data should be collected over a wide range of degradation cycles by executing run-to-failure tests. In fact, this is quite a costly process and is the price to pay for not having physics. The obtained data are used to train the model, which relates the h and u as inputs, and S and f_z as outputs. Same with the physics-based approach, the implementation consists of online diagnosis and offline prognosis. Online diagnosis is performed in two stages: estimation and prediction. The estimation stage is to input operation parameter u, measured feature f_z and system performance S to estimate the health parameter h of each component using the trained model, whereas the prediction stage is to input u and h to predict f_z and S. In the viewpoint of the algorithm, the prediction stage is simply to run the trained model, whereas the estimation stage requires a suitable algorithm that finds the input from the given output values. The off-line prognosis is the same as the physics-based approach: the health parameters are fitted by mathematical models, which are used to predict its degradation in the future. To this end, the $h_{0:k}$ estimated in the online diagnosis are transferred to the offline prognosis to fit the degradation model. Once the model is fitted, it is extrapolated to predict h in the future. The predicted h into the future is transferred to the offline diagnosis to predict the system performance S. Then they are transferred back to the online prognosis to obtain the future evolution of system performance. The overall procedure is summarized in Fig. 5, in which the highlighted parts are different from the physics-based approach.

III. CASE STUDY

A. PROBLEM STATEMENT

As stated before, it is hard to find field data for the system level PHM to study both the physics-based and data-driven approaches. Therefore, a DC motor system is considered, in which the virtual measurement data are generated by adding random noise to the simulation results. The DC motor converts electrical energy into mechanical power. When electric current passes through a coil in a magnetic field, the

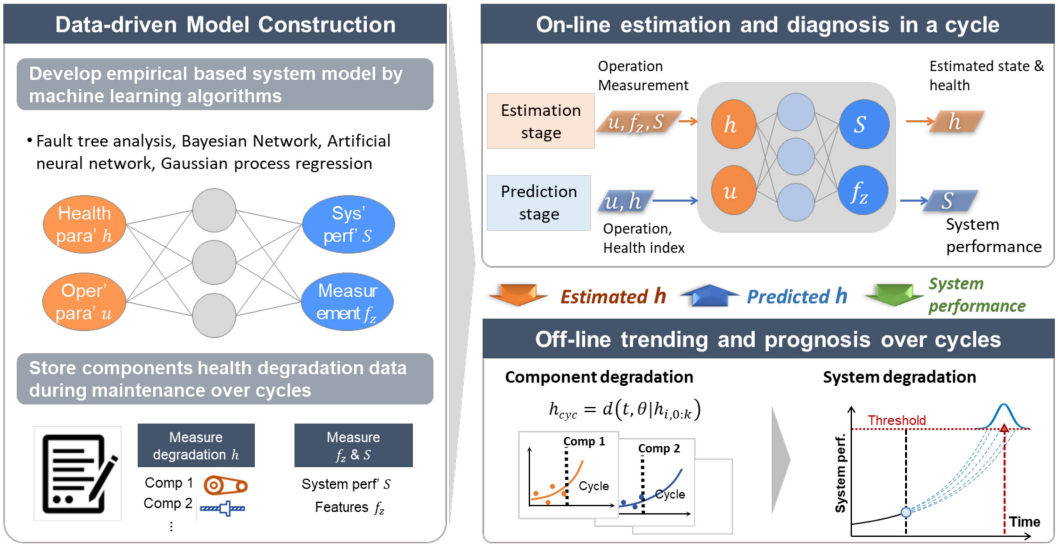

FIGURE 4. Architecture for a data-driven approach.

Construction phase (left figure)	
• Construct empirical based system model by machine learning algorithms using large amount of measured data for health parameter h, feature f_z and system performance S.	
Implementation phase (right figure)	
• Inversely estimate health parameter h using the measured f_z and S from the empirical model.	Estimation stage in upper figure
• Transfer estimated data $h_{0:k}$ up to the current cycle to offline trending.	
• Fit the data $h_{0:k}$ to degradation model (4) and extrapolate h to predict the future degradation.	Left part of lower figure
• Transfer predicted health parameters h in the future to online estimation.	
• Forwardly predict f_z and S using h in the future	Prediction stage in upper figure
• Transfer predicted S in the future to offline trending.	
• Determine the remaining life of S against failure threshold.	Right part of lower figure

Note the colored parts in the figure are different from data-driven approach.

FIGURE 5. Overall procedure for data-driven approach as illustrated in FIGURE 4.

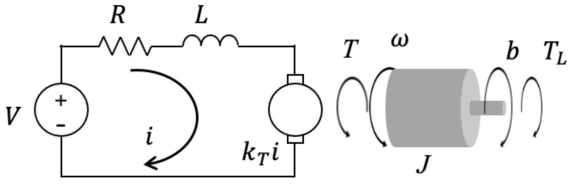

FIGURE 6. DC motor system.

magnetic force produces a torque that drives the DC motor. As shown in Fig. 6, the DC motor consists of the electrical and mechanical parts, in which they are coupled with each other. Therefore, failure in one part can affect the others. For example, since the magnetic flux converts the electrical energy into the mechanical force, its defect will deteriorate

TABLE 1. Parameter setting for simulation.

Symbol	Description	Value
R	Armature resistance	11.2 Ω
L	Armature inductance	0.1215 H
J	Moment of inertia	0.022145 kg m^2
b	Viscous friction coefficient	0.002953 N m s/rad
k_T	Electro-mechanical coupling coefficient	1.28 Nm/A
V	Input voltage	10 V
T_L	Load torque	0.05 Nm

the mechanical output. The mechanical and electrical parts of the DC motor dynamics are given by

$$J\frac{d\omega}{dt} + b\omega = k_T i - T_L = T_o \tag{6}$$

$$L\frac{di}{dt} + Ri = V - k_T\omega \tag{7}$$

where ω, i, and T_o represent the angular velocity, current, and output torque, respectively. The two equations share the common parameter k_T, which represents the electro-mechanical coupling coefficient. Table 1 explains parameters and their values used for the simulation [34]. The duration of a single cycle is 3 seconds, where the voltage of 10 V is applied for the first 1.5 seconds and then turned off for the rest. Figure 7 shows the time history of ω, i, and T_o as outputs from the dynamic equations in Eqs. (6) and (7). Angular velocity ω quickly increases to the desired value as the voltage is applied and decreases to zero after the voltage is turned off. Current i and output torque T_o suddenly rise to the peak at the start, followed by the gradual decrease until the voltage pulse ends, and show the reverse behavior when the voltage is turned off.

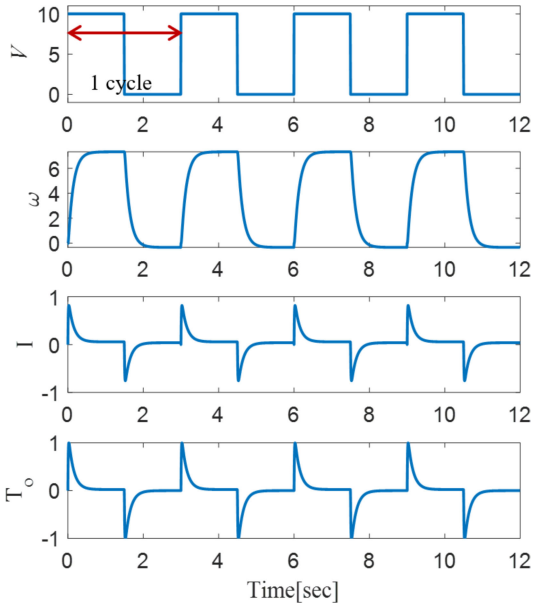

FIGURE 7. Simulation result of DC motor system.

B. SIMULATION OF COMPONENT DEGRADATION

One of the challenges of system-level prognosis is that multiple components degrade over time, which affects the system performance in a complex way. To simulate this situation, two components with associated failure modes are selected from the reference [35]. The first is the degradation of the permanent magnet due to prolonged overheating, which is also called flux weakening as it leads to the decrease in the magnetic field of the rotor. This can be described by decreasing the parameter, electro-mechanical coupling coefficient, k_T. The second is the loss of lubrication in the bearing, which can be modeled by a change in load torque T_L applied to the motor. The system performance is given by output torque, T_o, which may decrease as the two components degrade. The degradation behaviors of the magnet and bearing are assumed to be a linear and exponential function of cycles, respectively,

$$k_T(t) = \alpha_1 + \alpha_2 t \tag{8}$$

$$T_L(t) = \beta_1 e^{\beta_2 t} \tag{9}$$

where α_1 and β_1 represent the initial degradation state, while α_2 and β_2 describe the cycle-dependent behavior.

Three cases are considered as shown in Fig. 8: (1) degradation of the magnet with $\alpha_2 = -5.7974 \cdot 10^{-4}$, (2) degradation of the bearing with $\beta_2 = 3.3 \cdot 10^{-3}$, and (3) simultaneous degradation with the $\alpha_2 = -5.7974 \cdot 10^{-4}$ and $\beta_2 = 3.9 \cdot 10^{-3}$. In each case, the output torque is obtained by solving the system equations with the degraded values of k_T and T_L, as given in Figs. 8(a), (c) and (e). The results of output torque are given in Figs. 8(b), (d) and (f). In all cases, the maximum value of output torque gradually decreases as degradation proceeds, which indicates the degradation of system performance. In addition, when two components are degraded simultaneously as in Fig. 8(e), the system performance in Fig. 8(f) degrades faster than the single component degradation in Figs. 8(b) and 8(d).

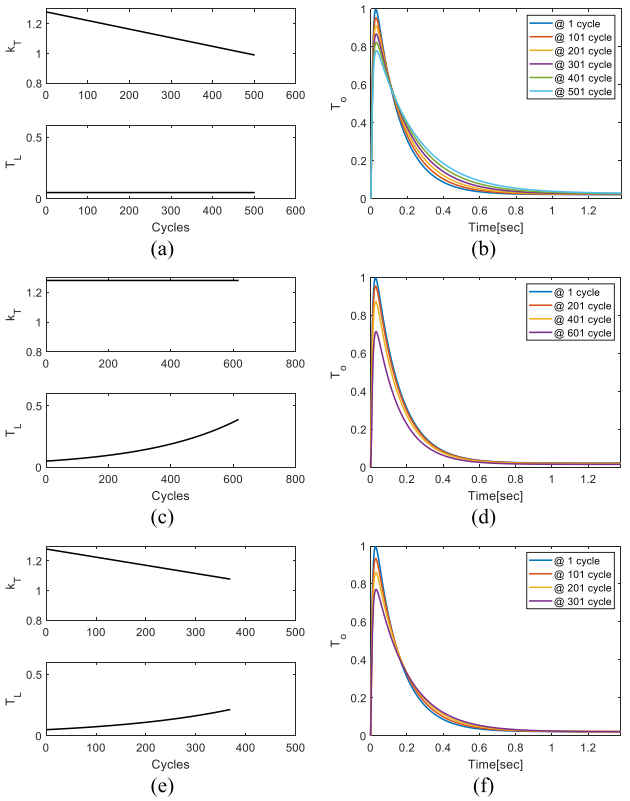

FIGURE 8. Output torque due to components degradation, (a) health parameters and (b) output torque of case 1, (c) health parameters and (d) output torque of case 2, and (e) health parameters and (f) output torque of case 3.

In this example, system performance S is defined by a scalar value, namely the maximum output torque:

$$S = maxT_0 = max(k_T i - T_L) \tag{10}$$

The system is regarded as a failure when the system performance decreases below 70% of its initial value. Therefore, it is necessary to predict how many cycles remain before failure, which component is responsible, and when it should be replaced.

IV. APPLICATION

A. APPLICATION OF PHYSICS-BASED APPROACH

As mentioned in the previous section, the first step of the physics-based approach is the construction of system dynamics model as shown in Eq. (1), where the state variable $\boldsymbol{x}$ (denoted by a vector hereafter) consists of velocity ω and current i, i.e., $\boldsymbol{x} = [\omega, i]^T$ while the input operation parameter u is voltage V. Health parameter $\boldsymbol{h}$ contains k_T and T_L or $\boldsymbol{h} = [k_T, T_L]^T$. Then the state model can be constructed from Eqs. (6) and (7) as

$$\begin{bmatrix} \dot{\omega} \\ \dot{i} \end{bmatrix} = \begin{bmatrix} -\frac{b}{J} & \frac{k_T}{J} \\ -\frac{k_T}{L} & -\frac{R}{L} \end{bmatrix} \begin{bmatrix} \omega \\ i \end{bmatrix} + \begin{bmatrix} -\frac{T_L}{J} \\ \frac{V}{L} \end{bmatrix} \tag{11}$$

Note that the equation describes the transient response of state variable $\boldsymbol{x}$. Since the state variable can be acquired during the operation from the control unit, the measurement model is given by

$$\boldsymbol{z} = \begin{bmatrix} 1 & 0 \\ 0 & 1 \end{bmatrix} \begin{bmatrix} \omega \\ i \end{bmatrix} + \boldsymbol{v} \tag{12}$$

where $\boldsymbol{z}$ is the measurement, and $\boldsymbol{v}$ is the zero-mean multivariate Gaussian noise. Measurement data are gathered with a 0.005 sec time interval.

Once the models are constructed, they are used for online estimation and diagnosis. In this study, the extended Kalman filter (EKF) algorithm is employed. In the estimation stage, the state variable is augmented by unknown health parameters $\boldsymbol{h}$, and denoted by $\boldsymbol{x} = \left[\boldsymbol{x}^T, \boldsymbol{h}^T\right]^T$ The state and measurement models in Eqs. (11) and (12) are rewritten into the recursive matrix form:

State model: $\boldsymbol{x}_t = F\left(\boldsymbol{x}_{t-1}\right) + \boldsymbol{w}_t$ or

$$\begin{bmatrix} \omega_t \\ i_t \\ k_{T,t} \\ T_{L,t} \end{bmatrix} = \begin{bmatrix} (1+b \cdot dt/J)\,\omega_t + dt/J(k_{T,t-1} \cdot i_{t-1} - T_{L,t-1}) \\ -dt/L \cdot k_{T,t-1} \cdot \omega_{t-1} + (1-R/L)\, i_{t-1} + -V \cdot dt/L \\ k_{T,t-1} \\ T_{L,t-1} \end{bmatrix} + \boldsymbol{w}_t \tag{13}$$

Measurement model: $\boldsymbol{z}_t = H\left(\boldsymbol{x}_t\right) + \boldsymbol{v}_t$ or

$$\boldsymbol{z}_t = \begin{bmatrix} 1 & 0 & 0 & 0 \\ 0 & 1 & 0 & 0 \end{bmatrix} \begin{bmatrix} \omega_t \\ i_t \\ k_{T,t} \\ T_{L,t} \end{bmatrix} + \boldsymbol{v}_t \tag{14}$$

where $k_{T,t}$ and $T_{L,t}$ denote the k_T and T_L at the current time t. Process error $\boldsymbol{w}_t$ is given by the zero-mean multivariate Gaussian noise with covariance whose diagonal elements are $10^{-9}vI$ where I is the identity matrix. Measurement noise $\boldsymbol{v}_t$ are set as 0.1 and 0.01 which can be found by evaluating the dispersion of measured data. More details for the EKF can be found in the literature (e.g., [36], [37]). The initial state variables are given as $\mathbf{x}_0 = [0, 0, 1.28, 0.05]^T$ based on the evaluation of k_T and T_L at the initial stage of motor operation. The estimation stage is processed in the two steps as shown in Fig. 2. The first is the prior estimation by the state model under a given input $\boldsymbol{u}$. Next is the posterior update by the measurement model, which leads to the estimated state variable and health parameters. Figs. 9(a) and (b) show the estimated state variable $\boldsymbol{x}$ (velocity and current) and health parameters $\boldsymbol{h}$ (k_T and T_L) along with 95% prediction and confidence intervals, respectively. As shown in Fig. 9(b), the health parameters quickly converge to the true value. The values at the end of the voltage application (i.e. 1.5 seconds) are then used as the estimated health of each component to assess the system performance given by Eq. (10).

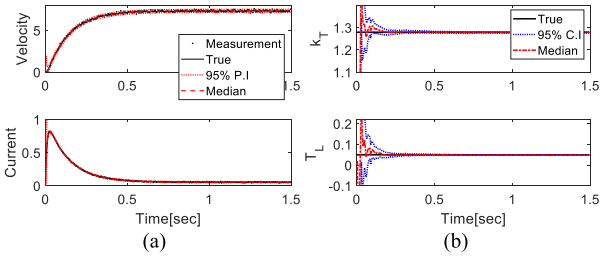

FIGURE 9. On-line estimation and diagnosis in a cycle by physics-based approach: (a) state variable x and (b) health parameters h.

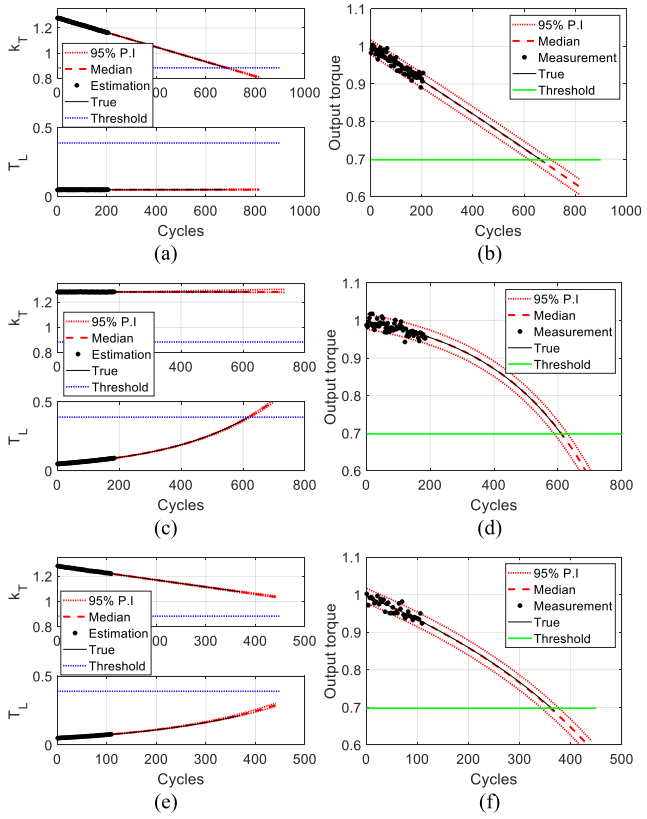

FIGURE 10. Off-line trending and prognosis over cycles by physics-based approach: (a) components health degradation for case 1, (b) system health degradation for case 1, (c) components health degradation for case 2, (d) system health degradation for case 2, (e) components health degradation for case 3 and (f) system health degradation for case 3.

Once the health parameters $\boldsymbol{h}$ are estimated at each cycle, the next step is to transfer them to the offline stage, as shown in Fig. 2. The results are given in Fig. 10(a), (c) and (e) for the three cases, in which the black dots denote health parameters estimated up to the current cycle. Using these data, the degradation models of each health parameter are fitted; that is, the model parameters $\boldsymbol{\alpha}$ and $\boldsymbol{\beta}$ in Eqs. (8) and (9) are estimated. For this purpose, Markov Chain Monte Carlo (MCMC) method [38] is used, which determines the parameters by a large number of samples (10^4 in this study) to account for the uncertainty due to the discrepancy between the data and the model. The degradation behaviors in the future are also predicted by extrapolating the model. In Fig. 10(a), (c) and (e), these are represented by the median and 95% predictive

interval (PI) curves. Note that the associated uncertainty is so small that they are nearly overlapped in this example. Once the health parameters $\boldsymbol{h}$ are predicted at the future cycles, they are transferred to the online stage in Fig. 2. In this case, they are used for the prediction stage, in which only the state variables $\boldsymbol{x}$ are estimated by the state model since $\boldsymbol{h}$ are known. Then the system performance at the future cycle is obtained as samples, which are transferred to the offline training part. The results are given by the median and 95% PI in Fig. 10(b), (d) and (f) for the three cases, respectively. It is worth noting that establishing the degradation model of system performance is not necessary since they are obtained from the online estimation stage as samples.

Since the true solutions are available, they are superposed by the solid black lines and compared with the predictions. The prediction results at the current cycle agree well with the true solutions for all the cases. It is noted that the system failure is defined as 70% of its initial value, which is depicted by the horizontal green line in the figure. Then the end of lives (EOLs) are found at 683, 617 and 369 cycles in terms of the median for the three cases. The reason for the shorter life in case 3 is because of the acceleration effect by the simultaneous degradation of both components. In Fig. 10(a) and (c) and (e), blue dotted horizontal lines indicate the failure thresholds of each health parameter. They are defined by the corresponding values at the EOL when the system undergoes degradation of each component. The threshold values for k_T and T_L are 0.8840 and 0.3897 at the EOLs 683 and 617 from cases 1 and 2, respectively.

Once we have the prognostic information for the system, one can evaluate the maintenance effect of individual components on the system health. The process is illustrated by case 3 where the two components degrade simultaneously. Note that if not stated otherwise, all the subsequent computations are based on the median values. At first, the current conditions are assessed by introducing the health index (HI) and the RUL. The HI indicates how healthy it is at the current condition, whereas the RUL estimates how many cycles remained until its failure. The HI is defined by the ratio of degradations at the current cycle versus at the EOL so that it ranges from 0 (normal) to 1 (failure). Since the k_T values at the initial, current, and EOL cycles are 1.28, 1.10, and 0.88 respectively (Fig. 10(a)), the index is (1.28-1.10)/(1.28-0.88) = 0.45. The indices for others can be obtained in the same way. The RUL is defined by the difference between the EOL and the current cycle. For k_T and T_L in Fig. 10(e), the EOLs are found at the cycles crossing the threshold lines (not shown here), which are about 721 and 513 respectively. Since the current cycle is 109, the RULs of k_T and T_L are about 609 and 412, and the system RUL is 361-109 = 252 cycles.

All the results are summarized in Table 2 and plotted by the bar charts in Fig. 11(a) and (b). Note in Table 2 that HI of k_T has degraded (increased) to 0.1507, greater (worse) than 0.0789 of T_L. But its RUL is about 609, which is longer than 412 of T_L. This is due to their different degree of contributions to the system performance.

TABLE 2. Parameter setting for simulation.

Name	Flux	Bearing	System performance
Symbol	k_T	T_L	S
Current cycle	109	109	109
End of life	718.0811	521.1807	361.0000
Remaining useful life	609.0811	412.1807	252.0000
Initial value	1.2796	0.0500	0.9971
Current value	1.2200	0.0768	0.9278
Threshold	0.8840	0.3897	0.6978

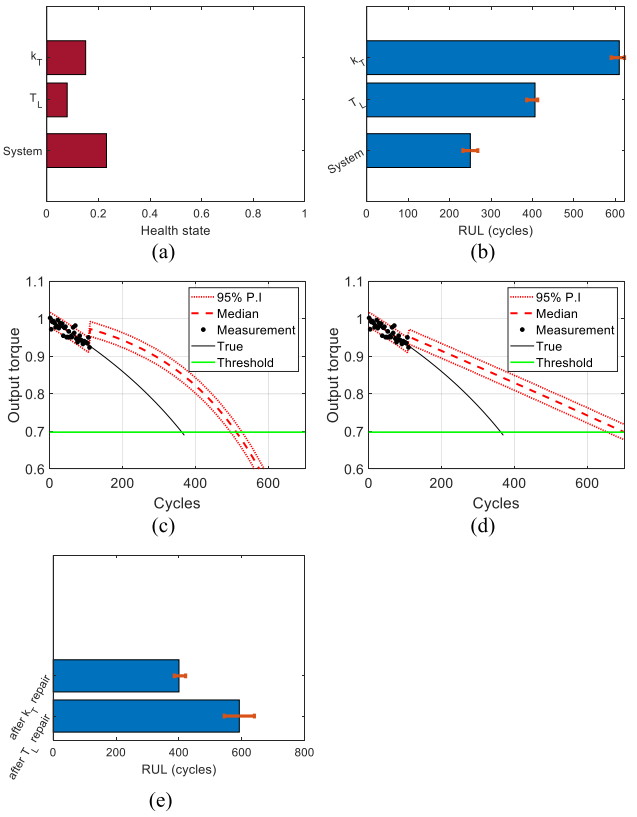

FIGURE 11. Maintenance scenario in physics-based approach: (a) current health state, (b) RUL of component and system, (c) prognosis with k_T repair, (d) prognosis with T_L repair and (e) system RUL when component is repaired.

Next, a what-if study is performed for the scenarios when one of the components is repaired or replaced by the new one. That is, the health parameter is reset to the original, and the system performance is predicted under the new condition. Results are given in Fig. 11(c) and (d) when the k_T and T_L are repaired respectively. The new EOLs are extended to about 512 and 701 cycles, yielding the new RULs around 403 and 592, respectively, as shown in Fig. 11(d). Among the two options of which component to repair, repairing T_L is more desirable, leading to the longer RUL. In Fig. 11(b) and (e), the red-colored error bar indicates the 95% PI of RUL prediction. From this study, several important information can be obtained: the current health condition of the components

and system, how long the system can be operated until failure, repairing which component is better to extend the system life longer, and how long it will be after repair.

B. APPLICATION OF DATA-DRIVEN APPROACH WITH MAINTENANCE INFORMATION

In the data-driven approach, it is necessary to have the health degradation data of the components and the system concurrently for the training, which we call 'labeled data'. It can be a quantitative measurement by appropriate device or at least subjective judgment by the maintenance personnel. For example, in this study, k_T and T_L can be obtained by measuring the electro-mechanical coupling coefficient and torque, respectively. In the real system, this can be best accomplished during periodic maintenance or by performing accelerated degradation tests. Both of them are costly or time-consuming processes, which is hard to achieve in practice. However, without having these data, it is difficult to perform data-driven prognostics, which is why the data-driven approach of the system is rare in the literature.

In the data-driven approach, measured data $\boldsymbol{z}$ is usually transformed into a set of scalar features f_z to reflect the health state of the components and system. Many signal processing techniques are available for this, among which the time-based features are most widely used. In this study, however, the values at 1.5 seconds, which is the end of the voltage-on period as shown in Fig. 9(a), are simply used as the features by intuition, based on the knowledge that they are influenced by the degradation of components over cycles.

In order to simulate the periodic inspection, parameters α_1 and β_1 are set as 1.28 Nm/A and 0.05 Nm, which correspond to the nominal states. The parameters α_2 and β_2 of the health parameters $\boldsymbol{h} = [k_T, T_L]$ in the degradation model in Eqs. (8) and (9) are randomly generated assuming the Gaussian distributions with $N(-7 \cdot 10^{-4}, 1.1 \cdot 10^{-4})$ and $N(4.8 \cdot 10^{-3}, 5 \cdot 10^{-4})$, respectively. Then the degraded health parameters are generated with the interval of 50 cycles from the degradation model. Using these values, the motor operation is simulated to get the measurement $\boldsymbol{z} = [\omega, i]$, their features $\boldsymbol{f}_z = [f_\omega, f_i]$ which denote the values at 1.5 seconds, and the system performance S (output torque). Then the measurement noises are added with the standard deviations 0.1, 0.001 and 0.01 to f_ω, f_i and S, respectively. Also, other noises are added to k_T and T_L with standard deviations 0.005 and 0.01 to simulate the measurement of component degradation during the periodic maintenance.

Ten datasets are generated for the three cases for training, as shown in the second column of Table 3. In the simulation, only two data sets are generated for case 3 since data under concurrent degradation of two components would be rare in real industry. Additional 3 datasets (one for each case) are generated for a test. As an example, a dataset for case 1 with the interval of 50 cycles is given in Fig. 12, which is the case that only k_T degrades. The configuration of training data is listed in Table 3. Using the 10 history datasets, 108 training

TABLE 3. Training data for each degradation case.

Degradation type	Num. of history data	Num. of measurements
Case 1	4	51
Case 2	4	42
Case 3	2	15

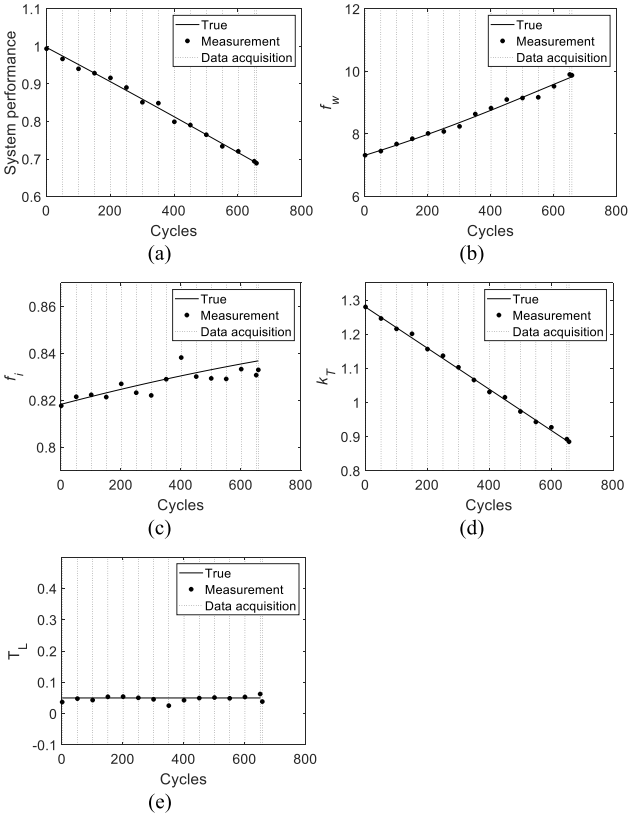

FIGURE 12. Training data measured at maintenance cycles for case 1 in data-driven approach: (a) system performance, (b) feature f_ω from velocity ω, (c) feature f_i from current i, (d) health parameter k_T, and (e) health parameter T_L.

data in total can be obtained, and they are used to train the system model as depicted in Fig. 3, which relates the measured performance S and features $\boldsymbol{f}_z$ as the output with the component health parameters $\boldsymbol{h}$ and operation parameter u as the input. The operation parameter u, however, which is the voltage in this problem, is not included as the input since it is constant all the time.

If the system is complex, preliminary work such as fault tree or Bayesian network analysis is necessary to identify the hierarchical causal effect relations between the components and system. Since the component's health, $\boldsymbol{h}$ affects the system performance, S and features $\boldsymbol{f}_z$, their causal relationship is represented with the Bayesian network as shown in Fig. 13. The figure indicates that three models should be constructed to relate the health condition, h with system performance, S, features, $\boldsymbol{f}_z$ (i.e. f_i and f_ω). Among many surrogate models, Gaussian process regression (GPR) is employed, which is to

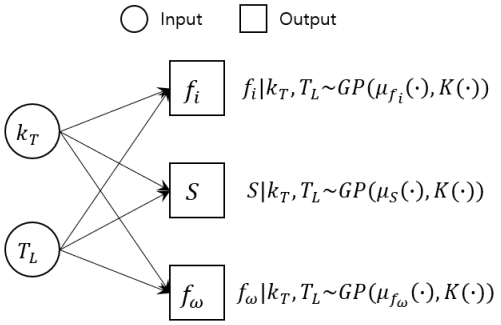

FIGURE 13. Bayesian network for the data-driven approach.

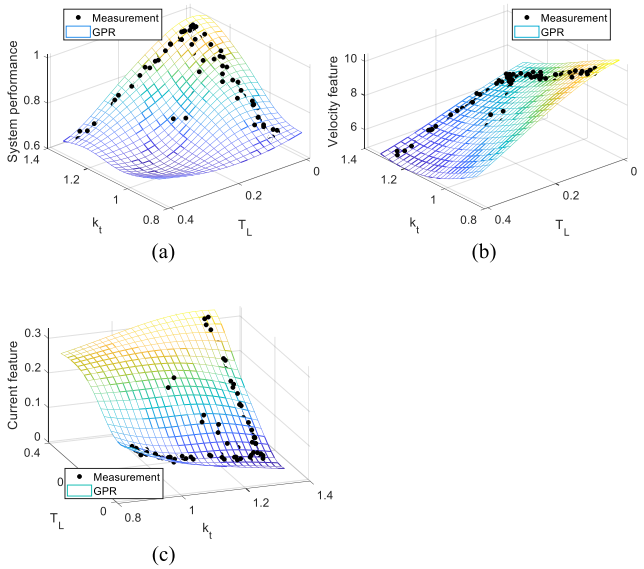

FIGURE 14. Gaussian process regression model as a function of k_T and T_L: (a) system performance S, (b) feature f_ω (velocity) and (c) feature f_i (current).

represent the probability density functions of S and $\boldsymbol{f}_z = [f_\omega, f_i]$, conditional on the observed data for $\boldsymbol{h} = [k_T, T_L]$. The $\mu(.)$ and $K(.)$ represent the mean and covariance matrix, respectively. The correlation function is defined by

$$K\left(x_i, x_j \,|\, \theta\right) = \sigma_f^2 exp\left[-\frac{1}{2}\sum_{m=1}^{d}\frac{(x_{im}-x_{jm})^2}{\sigma_m^2}\right] \quad (15)$$

where σ_f^2 and σ_m^2 are hyper-parameters associated with the scaling factor and length-scale, which are optimized based on the training data. The main advantage of the GPR over the ANN is that it can quantify the uncertainty of the model or measurement which is given by the predictive interval. More detailed descriptions of the GPR algorithm are available in [8]. The constructed GPR using the 10 training datasets are given by the surface plot in Fig. 14. Among 108 dots in the figure, those dots along the k_T and T_L axes denote case 1 and case 2, respectively, while those along the diagonal direction are case 3. The performance of GPR can be improved by uniformly filling data over the range, which means more measurements are needed. Once the GPRs are constructed,

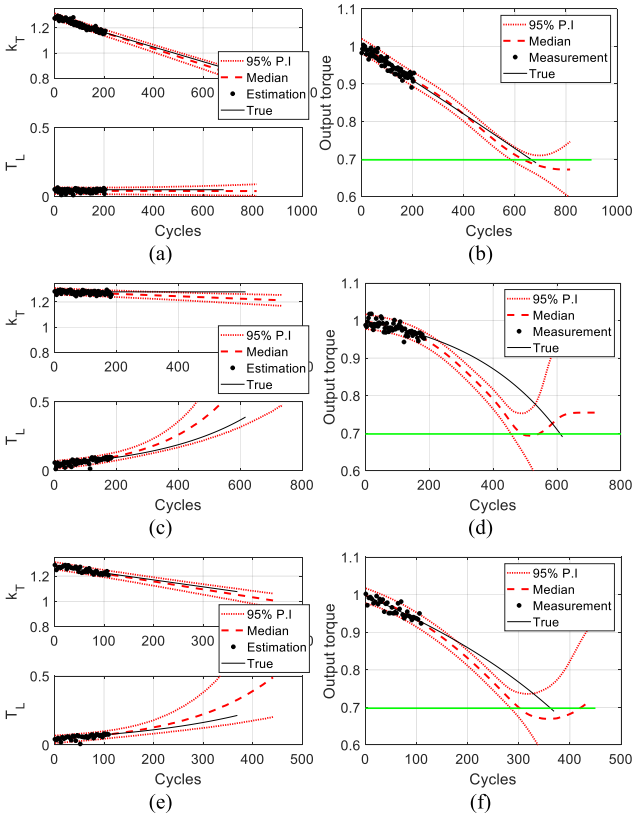

FIGURE 15. Off-line trending and prognosis over cycles by data-driven approach: (a) components health degradation for case 1, (b) system health degradation for case 1, (c) components health degradation for case 2, (d) system health degradation for case 2, (e) components health degradation for case 3 and (f) system health degradation for case 3.

they are used in the implementation phase given at the right side of Fig.4.

In order to validate the constructed model, the test datasets are used. In the online estimation stage, the health parameters $\boldsymbol{h}$ are estimated based on the measured features $\boldsymbol{f}_z$ and system performance S up to the current cycles (estimation stage). For this purpose, MCMC is performed to draw samples from the joint pdf of k_T and T_L which can be obtained based on the Bayesian theory using three GPR models (i.e. $f_i|k_T, T_L$, $f_\omega|k_T, T_L$, and $S|k_T, T_L$). Then, the median of $\boldsymbol{h}$ is transferred to the offline stage in Fig. 4, using which the degradation models are fitted in the same way as the physics-based approach. As a result, the degradation models and their extrapolation to the future are obtained by the samples, which are represented by the median and 95% PI as shown in Fig. 15 (a), (c) and (e) for the three cases respectively. Health parameter $\boldsymbol{h}$ obtained by the samples are transferred back to the online estimation stage in Fig. 4. For these samples as inputs, the GPR models are applied to predict the system performance S in the future (prediction stage). The results are given by the median and 95% PI in Fig. 15 (b), (d) and (f).

Comparing the results with the true solutions given by the solid black lines, the degree of agreement is less good than the physics-based approach. The PIs are wider too. Note however that the main point of the study is to suggest an

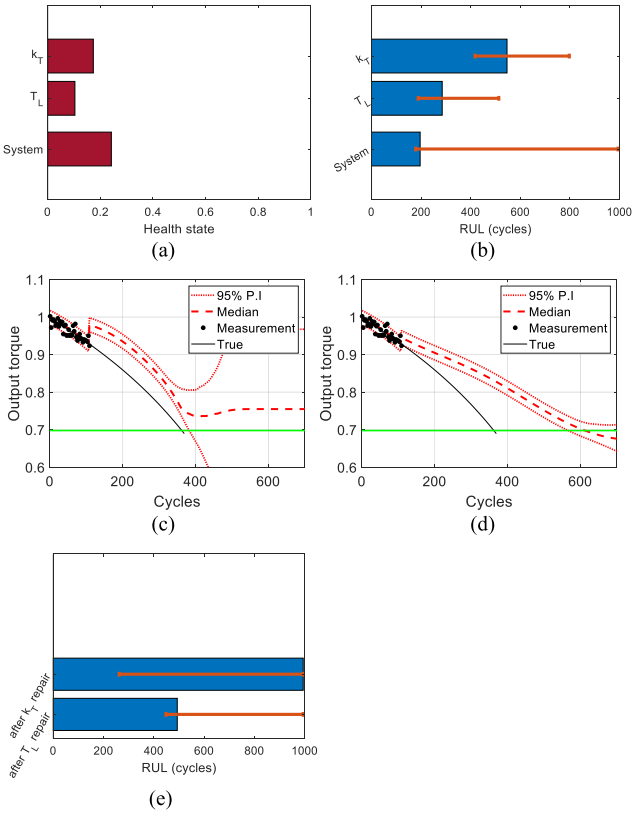

FIGURE 16. Maintenance scenario in data-driven approach: (a) current health state, (b) RUL of component and system, (c) prognosis with k_T repair, (d) prognosis with TL repair and (e) system RUL when the component is repaired.

adequate architecture for system-level PHM, by which the procedure can be easily implemented in general. Among the results of three cases, the predictions of system performance are inaccurate in cases 2(d) and 3(f) where the components degrade in a nonlinear way as in (c) and (e). This is typical for data-driven approaches, which is due to the lack of physics in the system model. Though not implemented here, however, it is anticipated that the accuracy will be improved as more data are added.

In conclusion, this approach also enables the same process as the physics-based approach that estimates the components' health condition and provides a future trajectory for system performance, which is considered an essential function for system-level PHM. The same process is conducted in the data-driven approach to evaluate the maintenance effect of individual components. As in the physics-based approach, case 3 is considered where the system performance is given by Fig. 15(f) due to the simultaneous degradation of the two components. For this case, current RULs are given in Fig. 16(b) along with PIs. When a component is replaced to its original condition, the new RULs are obtained and are given in Fig. 16(e). Among the results, the median and upper bound of the new RUL cannot be determined due to the poor prediction in these cycles. The predictions in Fig. 15(f) and 16(b) after 400 cycles are close to the constant value since the training data in that area did not exist. Nevertheless, it is reasonable to repair T_L since it gives longer RUL in terms of the lower bound. It shows that building high-quality physical or data-driven model that relates measurements to health condition of components and system performance is key ingredient for successful system-level prognostics. To avoid this and improve the results, more data are needed over the wider range of degradation cycles for training. Different kernel functions of the GPR may also help too. However, since the main scope is on the architecture of the System PHM not on solving the poor performance, this is not explored further.

V. DISCUSSIONS AND CONCLUSION

In the literature of PHM studies, many have investigated component-level problems. In the real field, however, the system-level PHM is of more importance, which explores the degradation of system health due to those of the components. The reason is evident that it is not feasible to replace the whole system when the system failure is predicted, but to replace only the responsible components. Examples can be found in many applications such as the semiconductor equipment or the gas turbine engine where the system cost is so prohibitive to replace it as a whole. In order to address this issue properly, the information for interaction between the component-level and the system-level degradation is crucial. This study has proposed appropriate architectures toward this end by two approaches: physics-based (Figs. 2 and 3) and data-driven prognostics (Figs. 4 and 5), which are demonstrated using a simple example of DC motor with two components.

The difference between the two architectures is in the model construction. In the physics-based approach, the relationship between the components and system is defined via the physics or dynamic model, while the data-driven approach uses a mathematical model. The data-driven approach requires a large number of run-to-fail data for feature f_z and system performance S over a wide range of cycles, which is considered as the major bottleneck for practice. On the other hand, the physical model is rarely available, which hinders the physics-based approach from the real field. Furthermore, the available physical model is often inaccurate, which requires substantial data and effort for verification and validation. In terms of the implementation, the physics-based approach requires only measurement z as the input, from which health parameter h as well as S are estimated. In addition to measurement z, the data-driven approach requires S as the input, from which health parameter h is estimated.

In the DC motor example, the physics-based approach uses transient measurement $\boldsymbol{z} = [\omega, i]$ to estimate $\boldsymbol{h} = [k_T, T_L]$ and S. The data-driven approach uses two features $\boldsymbol{f}_z = [f_\omega, f_i]$, which are $[\omega, i]$ at 1.5 seconds and S to estimate $\boldsymbol{h} = [k_t, T_L]$. Though not addressed in this study, in the viewpoint of real implementation, only one measurement out of $\boldsymbol{z} = [\omega, i]$ would be enough to estimate $\boldsymbol{h} = [k_T, T_L]$ in the physics-based approach. Analogously, only two out of three $[f_\omega, f_i, S]$ are enough in the data-driven approach to estimate the two health parameters $[k_T, T_L]$.

The uniqueness of the proposed architecture is that it enables the component-level prognosis result to be integrated into the system-level information. The system-level degradation model, which is usually used in the literature to predict its future behavior, is not necessary here. Instead, they are obtained from the component-level degradations, whose individual trends are defined by the degradation model. As a result, the architecture enables the estimation of components' health and that of the system, as well as the prediction of their RULs against the system failure threshold. Furthermore, a what-if study can be made to predict how long the system can be operated until failure by repairing each component, from which the maintenance plan can be made properly. However, it should be noticed that the decision-making on maintenance is not a simple task, considering, e.g., that repairing two components at once when they degrade closely might be better than to shut the system twice for individual repair. Another research is needed to make the optimum maintenance scheduling such as when to shut down, how many and which components to repair. It should account for the components health and RULs, their sensitivity to the system performance, and correlation to the other components degradation, and so on. Future works will contain two topics. First, a correlation between components. Correlation between components is one of the challenges of system-level prognostics. The current architecture will be extended to include the effect of correlation between components in the system. Second, architecture will be applied to a real industrial system which consists of multiple components such as DC motor, semiconductors, train door systems, or industrial robots.

REFERENCES

[1] J. Lee, F. Wu, W. Zhao, M. Ghaffari, L. Liao, and D. Siegel, "Prognostics and health management design for rotary machinery systems—Reviews, methodology and applications," *Mech. Syst. Signal Process.*, vol. 42, nos. 1–2, pp. 314–334, Jan. 2014, doi: 10.1016/j.ymssp.2013.06.004.

[2] B. Sun, S. Zeng, R. Kang, and M. G. Pecht, "Benefits and challenges of system prognostics," *IEEE Trans. Rel.*, vol. 61, no. 2, pp. 323–335, Jun. 2012, doi: 10.1109/TR.2012.2194173.

[3] D. Siegel, C. Ly, and J. Lee, "Methodology and framework for predicting helicopter rolling element bearing failure," *IEEE Trans. Rel.*, vol. 61, no. 4, pp. 846–857, Dec. 2012, doi: 10.1109/TR.2012.2220697.

[4] K. Medjaher, D. A. Tobon-Mejia, and N. Zerhouni, "Remaining useful life estimation of critical components with application to bearings," *IEEE Trans. Rel.*, vol. 61, no. 2, pp. 292–302, Jun. 2012, doi: 10.1109/TR.2012.2194175.

[5] C. Lim, S. Kim, Y.-H. Seo, and J.-H. Choi, "Feature extraction for bearing prognostics using weighted correlation of fault frequencies over cycles," *Struct. Health Monitor.*, vol. 19, no. 6, pp. 1808–1820, Nov. 2020, doi: 10.1177/1475921719900917.

[6] J. Park, S. Kim, J.-H. Choi, and S. H. Lee, "Frequency energy shift method for bearing fault prognosis using microphone sensor," *Mech. Syst. Signal Process.*, vol. 147, Jan. 2021, Art. no. 107068, doi: 10.1016/j.ymssp.2020.107068.

[7] J. Sim, S. Kim, H. J. Park, and J.-H. Choi, "A tutorial for feature engineering in the prognostics and health management of gears and bearings," *Appl. Sci.*, vol. 10, no. 16, p. 5639, Aug. 2020, doi: 10.3390/app10165639.

[8] R. R. Richardson, M. A. Osborne, and D. A. Howey, "Gaussian process regression for forecasting battery state of health," *J. Power Sources*, vol. 357, pp. 209–219, Jul. 2017, doi: 10.1016/j.jpowsour.2017.05.004.

[9] S. Kim, H. J. Park, J.-H. Choi, and D. Kwon, "A novel prognostics approach using shifting kernel particle filter of li-ion batteries under state changes," *IEEE Trans. Ind. Electron.*, vol. 68, no. 4, pp. 3485–3493, Apr. 2021.

[10] D. He, E. Bechhoefer, P. Dempsey, and J. Ma, "An integrated approach for gear health prognostics," in *Proc. AHS Int. 68th Annu. Forum Technol. Deip.*, Fort Worth, TX, USA, May 2012.

[11] M. E. Orchard and G. J. Vachtsevanos, "A particle-filtering approach for on-line fault diagnosis and failure prognosis," *Trans. Inst. Meas. Control*, vol. 31, nos. 3–4, pp. 221–246, Jun. 2009, doi: 10.1177/0142331208092026.

[12] S. Kim and J.-H. Choi, "Convolutional neural network for gear fault diagnosis based on signal segmentation approach," *Struct. Health Monitor.*, vol. 18, nos. 5–6, pp. 1401–1415, Nov. 2019.

[13] S. Park, S. Kim, and J.-H. Choi, "Gear fault diagnosis using transmission error and ensemble empirical mode decomposition," *Mech. Syst. Signal Process.*, vol. 108, pp. 262–275, Aug. 2018, doi: 10.1016/j.ymssp.2018.02.028.

[14] M. J. Daigle, A. Bregon, and I. Roychoudhury, "Distributed prognostics based on structural model decomposition," *IEEE Trans. Rel.*, vol. 63, no. 2, pp. 495–510, Jun. 2014, doi: 10.1109/TR.2014.2313791.

[15] M. Daigle and K. Goebel, "Multiple damage progression paths in model-based prognostics," in *Proc. Aerosp. Conf.*, Mar. 2011, pp. 1–10, doi: 10.1109/AERO.2011.5747574.

[16] A. S. S. Vasan, C. Chen, and M. Pecht, "A circuit-centric approach to electronic system-level diagnostics and prognostics," in *Proc. IEEE Conf. Prognostics Health Manage. (PHM)*, Jun. 2013, pp. 1–8, doi: 10.1109/ICPHM.2013.6621432.

[17] H. Khorasgani, G. Biswas, and S. Sankararaman, "Methodologies for system-level remaining useful life prediction," *Rel. Eng. Syst. Saf.*, vol. 154, pp. 8–18, Oct. 2016, doi: 10.1016/j.ress.2016.05.006.

[18] F. Tamssaouet, K. T. P. Nguyen, K. Medjaher, and M. E. Orchard, "Degradation modeling and uncertainty quantification for system-level prognostics," *IEEE Syst. J.*, vol. 15, no. 2, pp. 1628–1639, Jun. 2021, doi: 10.1109/JSYST.2020.2983376.

[19] F. Tamssaouet, K. T. P. Nguyen, and K. Medjaher, "System-level prognostics under mission profile effects using inoperability input–output model," *IEEE Trans. Syst., Man, Cybern. Syst.*, vol. 51, no. 8, pp. 4659–4669, Aug. 2021, doi: 10.1109/TSMC.2019.2944834.

[20] A. M. Riad, H. K. Elminir, and H. M. Elattar, "Evaluation of neural networks in the subject of prognostics as compared to linear regression model," *Int. J. Eng. Technol.*, vol. 10, no. 6, pp. 52–58, 2010.

[21] M. Abbas, "System level health assessment of complex engineered processes," Ph.D. dissertation, Georgia Inst. Technol., Atlanta, GA, USA, 2010.

[22] L. Wen, Y. Dong, and L. Gao, "A new ensemble residual convolutional neural network for remaining useful life estimation," *Math. Biosci. Eng.*, vol. 16, no. 2, pp. 862–880, 2019, doi: 10.3934/mbe.2019040.

[23] F. O. Heimes, "Recurrent neural networks for remaining useful life estimation," in *Proc. Progn. Heal. Manag. Int. Conf. (PHM)*, Oct. 2008, pp. 1–6, doi: 10.1109/PHM.2008.4711422.

[24] Y. Wu, M. Yuan, S. Dong, L. Lin, and Y. Liu, "Remaining useful life estimation of engineered systems using vanilla LSTM neural networks," *Neurocomputing*, vol. 275, pp. 167–179, Jan. 2018, doi: 10.1016/j.neucom.2017.05.063.

[25] S. Zheng, K. Ristovski, A. Farahat, and C. Gupta, "Long short-term memory network for remaining useful life estimation," in *Proc. IEEE Int. Conf. Prognostics Health Manage. (ICPHM)*, Jun. 2017, pp. 88–95.

[26] C. S. Hsu and J. R. Jiang, "Remaining useful life estimation using long short-term memory deep learning," in *IEEE Int. Conf. Appl. Syst. Invention (ICASI)*, Apr. 2018, pp. 58–61, doi: 10.1109/ICASI.2018.8394326.

[27] J. Sun, H. Zuo, W. Wang, and M. G. Pecht, "Application of a state space modeling technique to system prognostics based on a health index for condition-based maintenance," *Mech. Syst. Signal Process.*, vol. 28, pp. 585–596, Apr. 2012, doi: 10.1016/j.ymssp.2011.09.029.

[28] T. Wang, J. Yu, D. Siegel, and J. Lee, "A similarity-based prognostics approach for remaining useful life estimation of engineered systems," in *Proc. Int. Conf. Prognostics Health Manage.*, Oct. 2008, pp. 1–6, doi: 10.1109/PHM.2008.4711421.

[29] T. Wang, "Trajectory similarity based prediction for remaining useful life estimation," Ph.D. dissertation, Dept. Ind. Eng., Univ. Cincinnati, Cincinnati, OH, USA, Aug. 2010.

[30] C. Hu, B. D. Youn, P. Wang, and J. T. Yoon, "Ensemble of data-driven prognostic algorithms for robust prediction of remaining useful life," *Rel. Eng. Syst. Saf.*, vol. 103, pp. 120–135, Jul. 2012, doi: 10.1016/j.ress.2012.03.008.

[31] S. Kim, N. H. Kim, and J.-H. Choi, "Prediction of remaining useful life by data augmentation technique based on dynamic time warping," *Mech. Syst. Signal Process.*, vol. 136, Feb. 2020, Art. no. 106486.
[32] C. Hu, B. D. Youn, T. Kim, and P. Wang, "A co-training-based approach for prediction of remaining useful life utilizing both failure and suspension data," *Mech. Syst. Signal Process.*, vols. 62–63, pp. 75–90, Oct. 2015, doi: 10.1016/j.ymssp.2015.03.004.
[33] C. Sobie, C. Freitas, and M. Nicolai, "Simulation-driven machine learning: Bearing fault classification," *Mech. Syst. Signal Process.*, vol. 99, pp. 403–419, Jan. 2018, doi: 10.1016/j.ymssp.2017.06.025.
[34] X. Zhu, H. Zhang, J. Xi, J. Wang, and Z. Fang, "Robust speed synchronization control for clutchless automated manual transmission systems in electric vehicles," *Proc. Inst. Mech. Eng., D, J. Automobile Eng.*, vol. 229, no. 4, pp. 424–436, Mar. 2015, doi: 10.1177/0954407014546431.
[35] T. Salem and T. A. Haskew, "Simulation of the brushless DC machine," in *Proc. 27th Southeastern Symp. Syst. Theory*, 1995, pp. 18–22.
[36] R. K. Singleton, E. G. Strangas, and S. Aviyente, "Extended Kalman filtering for remaining-useful-life estimation of bearings," *IEEE Trans. Ind. Electron.*, vol. 62, no. 3, pp. 1781–1790, Mar. 2015, doi: 10.1109/TIE.2014.2336616.
[37] V. A. Bavdekar, A. P. Deshpande, and S. C. Patwardhan, "Identification of process and measurement noise covariance for state and parameter estimation using extended Kalman filter," *J. Process Control*, vol. 21, no. 4, pp. 585–601, Apr. 2011, doi: 10.1016/j.jprocont.2011.01.001.
[38] N.-H. Kim, D. An, and J.-H. Choi, *Prognostics and Health Management of Engineering Systems*. Cham, Switzerland: Springer, 2017.

SEOKGOO KIM received the bachelor's and master's degrees in mechanical engineering from Korea Aerospace University, Goyang-si, South Korea, in 2016 and 2018, respectively. He is currently pursuing the dual Ph.D. degree with Korea Aerospace University and the University of Florida. His research interests include prognostics and health management for complex engineering systems, data analytics, machine learning, and uncertainty management. He has received the KSME Student Best Paper Award, in 2019, the ICMR Best Paper Award, in 2019, and the PHM Asia Pacific Best Student Award (Bronze), in 2021.

NAM HO KIM received the Ph.D. degree from the Department of Mechanical Engineering, The University of Iowa, in 1999. He worked at the Center for Computer-Aided Design as a Postdoctoral Associate, until 2001. He is currently a Professor of mechanical and aerospace engineering with the University of Florida. His research interests include design under uncertainty, prognostics, and health management, verification validation, and uncertainty quantification. He has published seven books and more than 200 refereed journals and conference papers in the above areas.

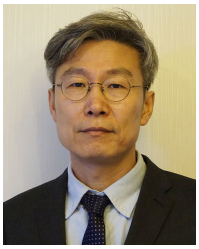

JOO-HO CHOI received the B.S. degree in mechanical engineering from Hanyang University and the M.S. and Ph.D. degrees in mechanical engineering from the Korea Advanced Institute of Science and Technology, Seoul, South Korea. He has worked as an Engineer with Samsung Corning, Suwon-si, South Korea, in which he has led the research team developing equipment to improve quality and productivity in TV glass production. He is currently a Professor of aerospace and mechanical engineering with Korea Aerospace University, Goyang-si, South Korea. Over the years, he has made some key publications including the reviews, tutorials, and a book to help the engineers' research and practice in the field of prognostics and health management (PHM). He founded the Korea Society for PHM, South Korea. In 2018, he was awarded the fellow from the PHM Society of USA for his leadership as the Chair in the first Asia Pacific Conference of the PHM Society 2017. He has served as an Editor for the *Journal of Mechanical Science and Technology* for six years.